Langmuir
Article
pubs.acs.org/Langmuir

Nanostructured Colloidal Crystals from Forced Hydrolysis Methods

Eugenio H. Otal,*,† Mara Granada,‡ Horacio E. Troiani,‡ Horacio Cánepa,† and Noemí E. Walsöe de Reca†

†*CINSO, Centro de Investigaciones en Sólidos, CONICET, CITEFA, San Juan Bautista de La Salle 4397, (B1603ALO) Villa Martelli, Buenos Aires, Argentina, and* ‡*Centro Atómico Bariloche (CNEA) and Instituto Balseiro (UNCuyo), (R8402AGP) San Carlos de Bariloche, Rio Negro, Argentina*

Received March 5, 2009. Revised Manuscript Received May 1, 2009

In this work, an original route for ZnO nanostructured spherical colloids and their assembly into colloidal crystals are presented. The temporal evolution of crystal size and shape was followed by X-ray diffraction and the colloids size distribution by scanning electron microscopy. These spherical colloids showed a change in their size dispersion with aging time. Early stage suspensions, with a narrow size distribution, were settled to the bottom and dried with a slow evaporation rate to obtain colloidal crystals. This original route provides a new material for future applications in opalline photonic crystals, with a dielectric constant higher than that of classical materials (silica and latex). Moreover, this route means an improvement of previously reported data from the literature since it involves a one-pot strategy and room-temperature colloid assembly.

1. Introduction

The strong interest in nanosized semiconductors is associated with their tunable band gap resulting from quantum confinement.[1] The control of synthesis parameters to grow new materials with fixed morphological properties like grain size and crystalline structure is useful for many applications, including photovoltaic cells based on low-cost materials,[2] hybrid organic−inorganic light-emitting devices,[3] telecommunication amplifier nanocrystals in which the luminescence band can be tailored to requirements by modification of the crystal size, nanostructured photonic crystals,[4] and thin film sensors.[5]

The II−VI semiconductor ZnO is environmentally friendly and easy to obtain from polar solvents in nanometric dimensions. It exhibits a high dielectric constant (3.75),[6] a wide band gap, and a large exciton binding energy (60 meV).[7] It crystallizes in the $P6_3mc$ space group, acquiring anisotropic growth properties that allow needles, tetrapods, nanorods, shells, ribbons, and highly faceted rods to be obtained.[8] All the different morphologies and properties make ZnO a good candidate for the above-mentioned applications.

These materials exhibiting a high dielectric constant and binding energy are, doubtless, convenient choices for optic applications as laser[9] and photonic crystals.[10] Solid state light-pumped lasers have been reported,[11] in spite of the fact that electrically pumped lasing has not yet been achieved, and a few works on applications in photonic crystals have been published.[10]

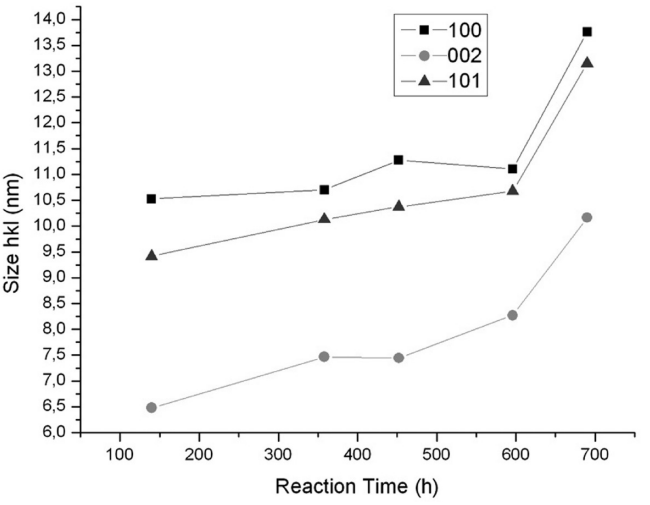

Figure 1. Variation of crystal size with reaction time obtained from XRD peaks corresponding to different crystalline directions: [100] (*a*-axis), [002] (*c*-axis), and [101].

Herein, we report a procedure for the preparation of nanostructured ZnO colloids and their self-assembly producing higher-order hierarchical structures.

2. Experimental Section

Synthesis. The procedure of this work is based on the routes reported by Bao et al.[12] and Ohyama et al.[13] for *c*-axis highly textured films, modified to obtain nanostructured ZnO colloids.

Materials. Zinc acetate dehydrate (puriss) (ZAD) and absolute ethanol (p.a.) (Merck) and diethanolamine (DEA) (p.a., ACS) (J. T. Baker) were used without further purification.

*To whom correspondence should be addressed. E-mail: eotal@citefa.gov.ar. Telephone: 54-11-4709 8100, ext. 1317. Fax: 54-11-4709 8228.

(1) Brus, L. *Appl. Phys. A: Mater. Sci. Process.* **1991**, 53, 465.
(2) Martinez, M. A.; Herrero, J.; Gutiérrez, M. T. *Sol. Energy Mater. Sol. Cells* **1997**, 45, 75.
(3) Bolink, H. J.; Coronado, E.; Repetto, D.; Sessolo, M. *Appl. Phys. Lett.* **2007**, 91, 223501.
(4) Scharrer, M.; Wu, X.; Yamilov, A.; Cao, H.; Chang, R. P. H. *Appl. Phys. Lett.* **2005**, 86, 151113.
(5) Mitra, P.; Chatterjee, A. P.; Maiti, H. S. *Mater. Lett.* **1998**, 35, 33.
(6) Landolt-Börnstein. *New Series, Group III*; Springer: Heidelberg, Germany, 1999; Vols. *17B, 22, 41B*.
(7) Ozgür, U.; Alivov, Ya. ; Liu, C.; Teke, A; Rehchikov, M. A.; Doğan, S.; Avrutin, V.; Cho, S. J.; Morkoç, H. *J. Appl. Phys.* **2005**, 98, 041301.
(8) Djurišić, A.; Leung, Y. H. *Small* **2006**, 2, 944.
(9) Bagnall, D. M.; Chen, Y. F.; Zhu, Z.; Yao, T.; Koyama, S.; Shen, M. Y.; Goto, T. *Appl. Phys. Lett.* **1997**, 70, 2230.
(10) Seelig, E. W.; Tang, B.; Yamilov, A.; Cao, H.; Chang, R. P. H. *Mater. Chem. Phys.* **1993**, 80, 257.
(11) Tang, Z. K.; Wong, G. K. L.; Yu, P.; Kawasaki, M.; Ohtomo, A.; Koinuma, H.; Segawa, Y. *Appl. Phys. Lett.* **1998**, 72, 3270.
(12) Bao, D.; Gu, H.; Kuang, A. *Thin Solid Films* **1998**, 312, 37.
(13) Ohyama, M.; Kouzuka, H.; Yoko, T. *Thin Solid Films* **1997**, 306, 78.

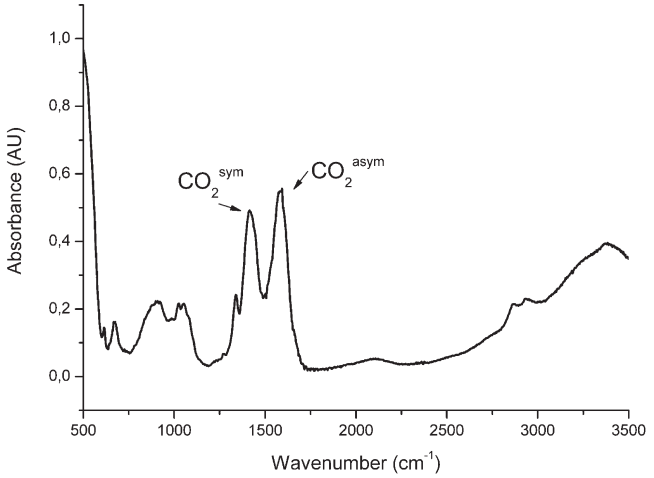

Figure 2. FTIR spectrum of colloids dried at room temperature.

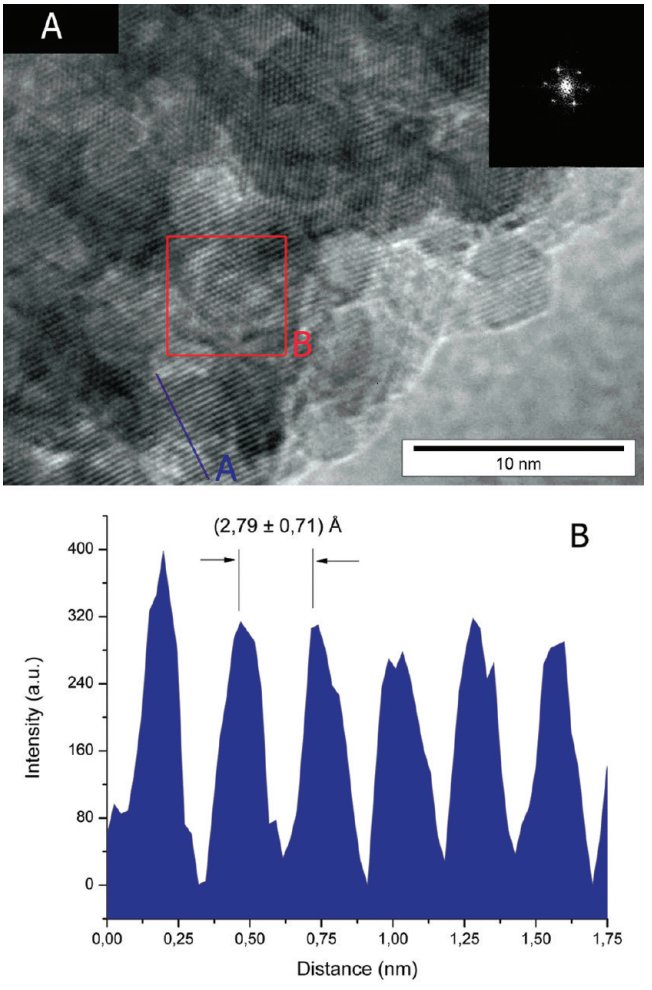

Figure 3. (a) HRTEM micrograph of the border of colloids after reaction for 140 h. In the inset, the fast Fourier transform of the square zone B is shown. (b) Intensity vs distance among planes taken on line A of panel a.

Precursor Solution (PS) Preparation. ZAD (2.19 g, 0.1 mol) was suspended in 100 mL of absolute ethanol. Anhydrous zinc acetate precipitates are dissolved after a few minutes under reflux, giving a 100 mmol/L solution. The solution was refluxed for 1 h and afterward cooled to room temperature.

Basic Complexation Solution (BCS) Preparation. To obtain a 100 mmol/L solution of DEA, 10.5 g (0.01 mol) of DEA was dissolved in 100 mL of absolute ethanol and the mixture stirred until a homogeneous solution was obtained.

Figure 4. Selected area electron diffraction pattern (SAED) of a single colloid.

Reaction Solution Preparation. Equal volumes of PS and BCS were mixed at room temperature. The DEA:Zn ratio was kept at 1.0, the final concentration in the solution being 50 mmol/L. This reaction mixture was placed in a 250 mL Schott Duran glass bottle closed with a Teflon-modified screw cap to maintain the inner pressure. The bottles were kept at 70 °C in a closed oven until turbidity appeared.

Sample Isolation. The turbid solution was cooled to room temperature and centrifuged at 2000 rpm. The solution was discarded, and the resulting solid was washed, suspended in ethanol (96°, tech. grade), and centrifuged to eliminate residual DEA and acetate. The obtained powder was dried in air at atmospheric pressure.

Colloidal Crystal Production. Glassware was cleaned overnight in a potassium hydroxide isopropylic alcohol solution. The colloid suspension was kept in a clean test tube at room temperature, covered with Parafilm to decrease the rate of solvent evaporation. As the solvent was completely eliminated, an iridescent residue was obtained at the bottom of the tube.

Characterization Methods. A PW 3710 Phillips diffractometer was used for X-ray diffraction (XRD) measurements. The instrumental broadening was corrected with a LaB_6 standard. Samples and standards were measured in Bragg−Brentano configuration in the range of 20−100° with a step of 0.02°. Transmission electron microscopy (TEM) images and electron diffraction patterns where obtained with a Philips CM200 microscope in an ultratwin objective lens using an operating voltage of 200 kV. Infrared spectra were recorded in a Nicolet model 520-P Fourier transform infrared spectrometer. Scanning electron microscopy (SEM) analysis was performed with a Karl Zeiss FESEM DSM 982 Gemini instrument.

3. Results and Discussion

The first step of the reaction consists of the transformation from primary particles of zinc acetate complexes to ZnO nanoparticles

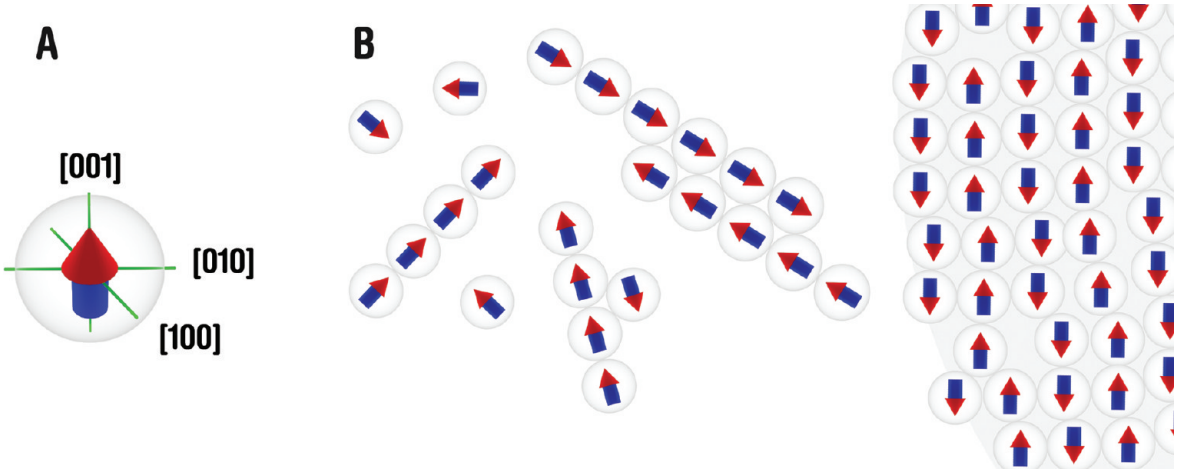

Figure 5. (A) Scheme of a nanoparticle with its main crystalline axes and dipole orientation. (B) Simplified mechanism of crystallite agglomeration, from monomer to chains, more complex chains, and finally colloids (in a 2D projection).

a few nanometers in size. The second step consists of the formation of secondary particles with a diameter of some hundreds of nanometers by the agglomeration of primary particles. The size of primary particles increases monotonically with reaction time, whereas the dimension of secondary particles exhibits at the beginning a sharp monodispersion and later a broadening in size distribution.

The reaction is conducted in absolute ethanol; the small amount of water for the hydrolytic processes comes from the hydration water of the inorganic precursor salt, zinc acetate dihydrate (ZAD). Additional water is provided by the condensation reaction between acetate and ethanol that occurs gradually during the formation of particles.

Too much water increases the crystal size, while a lack of water does not allow the hydrolysis process or formation of nanocrystals. Consequently, the water content contributes to control both situations in the formation of nanocrystals.

The complex hydrolysis reaction starts with the formation of primary clusters during the dissolution of ZAD in ethanol:[14]

$$4Zn(AcO)_2 \cdot 2H_2O \rightarrow Zn_4O(AcO)_6 + 7H_2O + 2HAcO$$

A primary cluster is slightly more stable than ZAD in the presence of water, but it also reacts with water, forming Zn-OH and AcOH. The control over all these processes is carried out by the action of diethylamine (DEA), which contributes with OH− to the medium and forms a soluble $Zn(DEA)_2^{2+}$ complex retarding the delivery of free ions to the solution.[15] Moreover, acetate groups protect the surface as a capping agent. Similar results with respect to the particle dimension and shape of ZnO nanoparticles are obtained, regardless the addition of a strong noncomplexing base[16] or a weak complexing one. However, the use of a weak complexing base is advantageous in two fundamental aspects. (1) It offers the possibility of following the kinetics of particle formation and stopping it at a desired time and tuning the optical properties of material, and (2) the slow formation of nanocrystals allows the agglomeration of secondary particles which is not controlled by diffusion but by reaction (these results are discussed below).

There are two ways of studying the nanocrystal growth kinetic: UV−vis spectroscopy (if the solution is clear) or once the precipitates have been obtained by the peak broadening in XRD patterns. Besides, it is interesting to know the nanocrystal size once the secondary colloids are obtained, in which case XRD is the appropriate technique, UV−vis spectroscopy being not useful because of the opacity of the solution. The kinetic study was conducted on six samples extracted at different times during the reaction, which were dried to yield a solid to be analyzed by XRD. The resulting particle size for different reaction times was determined by using the Scherrer equation:[17]

$$d = \frac{0.94\lambda}{\cos\theta\sqrt{\mathrm{FWHM}^2 - \mathrm{FWHM}_0{}^2}}$$

The broadening of peak technique was used, applying the correction for instrumental broadening ($FWHM_0$). The broadening of the peaks corresponding to [100], [002], and [101] diffractions was considered to gain information about a possible preferential direction growth (Figure 1). The (100) plane is considered as a nonpolar and stable face, while the (001) plane is a polar one; therefore, differences could be found in the growth rate ($V_{001} > V_{100}$).[18] The stabilization of polar faces can be achieved by crystallographic rearrangement, showing a massive surface reconstruction or exhibiting faceting to accommodate the charge transfer. Adsorbed molecules can also reduce the instability[19] like acetates, which in this case act as a capping agent. This result was confirmed by FTIR measurements, exhibiting bands of $CO_2{}^{sym}$ at 1414 cm^{-1} and $CO_2{}^{antisym}$ at 1586 cm^{-1} (Figure 2). The mode of binding of acetate to the ZnO is not clear, as there is not enough information to decide between a bidentate or chelate binding mode. However, unidentate binding can be ruled out because the shift among the symmetrical and antisymmetrical carboxy late bands, of 172 cm^{-1}, is not sufficiently large.[20] No bands evidencing the presence of DEA were found in the solid, a reasonable fact because of the solubility of $Zn(DEA)_2^{2+}$ in the presence of acetate as a counterion (a complete list of solids and soluble complexes is reported in ref 18). The obtained

(14) Tokumoto, M. S.; Briois, V.; Santilli, C. V.; Pulcinelli, S. H. *J. Sol-Gel Sci. Technol.* **2003**, 26, 547.
(15) Varadan, R.; Sriman, S.; Rao, V. R. S. *J. Radioanal. Nucl. Chem.* **1984**, 87, 23.
(16) Spanhel, L.; Anderson, M. A. *J. Am. Chem. Soc.* **1991**, 113, 2826.
(17) Tibbetts, G. G.; Sachdev, A. K.; Wims, A. M.; Franetovic, V. *J. Mater. Sci.* **1999**, 34, 1017.
(18) Li, W.-J.; Shi, E.-W.; Zhong, W.-Z.; Yin, Z.-W. *J. Cryst. Growth* **1999**, 203, 186.
(19) Meyer, B.; Marx, D. *Phys. Rev. B* **2003**, 67, 035403.
(20) Deacon, G. B.; Phillips, R. J. *Coord. Chem. Rev.* **1980**, 33, 227.

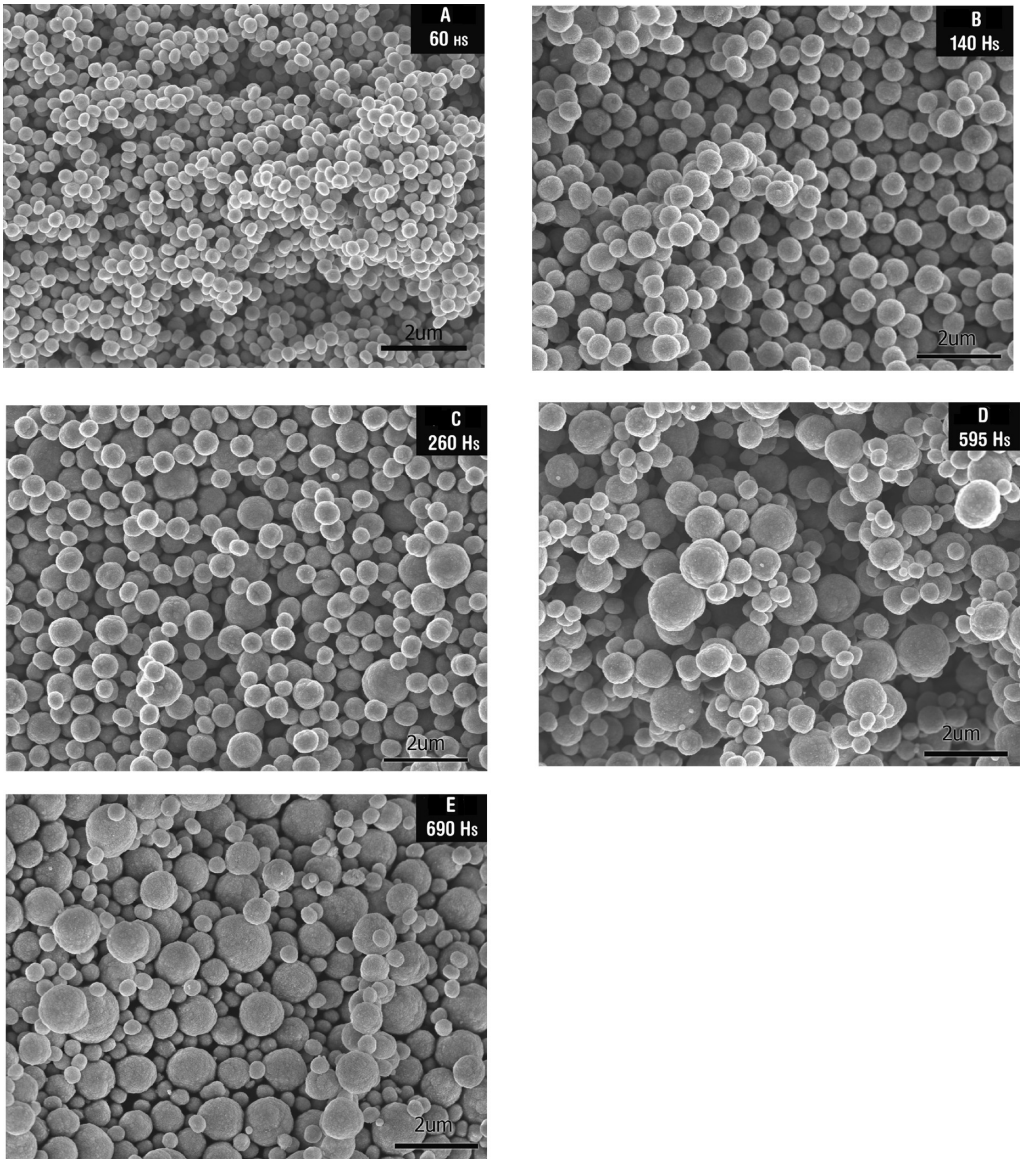

Figure 6. SEM micrographs of samples with different reaction times: (a) 60, (b) 140, (c) 260, (d) 595, and (e) 690 h.

particles might have a faceted flakelike shape,[21] exhibiting a contraction along the *c*-axis. It is also known that the peak broadening can be attained by size reduction and stress in the crystal.[22]

TEM images of these samples show that the colloids are formed by agglomeration of crystallites. Figure 3A is a high-resolution TEM image of the border of a particle, showing that the atomic planes of all the crystallites are well-oriented. Selected area diffraction (SAED) patterns of single colloids (Figure 4) confirm that the crystallites composing them are not randomly oriented, but they agglomerate with nearly the same orientation. The intensity profile over line A that crosses the planes parallel to the surface of the colloids (Figure 3B) shows a periodicity corresponding to the distance between planes (100).

The crystalline orientation of the building blocks composing the colloids can be explained by the high dipolar moment of wurtzite, parallel to the *c*-axis.[23] The orientation phenomenon also induces the formation of several other structures like chains[24] and two-dimensional (2D) arrays[25] of nanoparticles. The origin of these dipoles in the wurtzite crystal structure[24,26] has been attributed to the presence of surface-localized charges along the *c*-axis, the inner bonding geometry, the shape asymmetry, and the surface strain.[27,28]

The initial stages of colloid formation are driven by dipolar interactions between nanocrystals that form short chains, which grow by addition of monomers and/or other chains. The agglomeration proceeds until the spheres are formed. A simplified scheme of the nano building blocks and the process of agglomeration is shown in Figure 5. It was reported that the

(21) Audebrand, N.; Auffredic, J. P.; Louer, D. *Chem. Mater.* **1998**, 10, 2450.
(22) Klug, H. P.; Alexander, L. E. *X-ray diffraction procedures for polycrystalline and amorphous materials*, 2nd ed.; John Wiley: London, 1974.
(23) Nann, T.; Schneider, J. *Chem. Phys. Lett.* **2004**, 384, 150.
(24) Klokkenburg, M.; Houtepen, A. J.; Koole, R.; de Folter, J. W. J.; Erné, B. H.; van Faassen, E.; Vanmaekelbergh, D. *Nano Lett.* **2007**, 7, 2931.
(25) Talapin, D. V.; Shevchenko, E. V.; Murray, C. B.; Titov, A. V.; Král, P. *Nano Lett.* **2007**, 7, 1213.
(26) Sinyagin, A. Y.; Belov, A.; Tang, Z.; Kotov, N. A. *J. Phys. Chem. B* **2006**, 110, 7500.
(27) Shim, M.; Guyot-Sionnest, P *J. Chem. Phys.* **1999**, 111, 6955.
(28) Rabani, E. *J. Chem. Phys.* **2001**, 115, 1493.

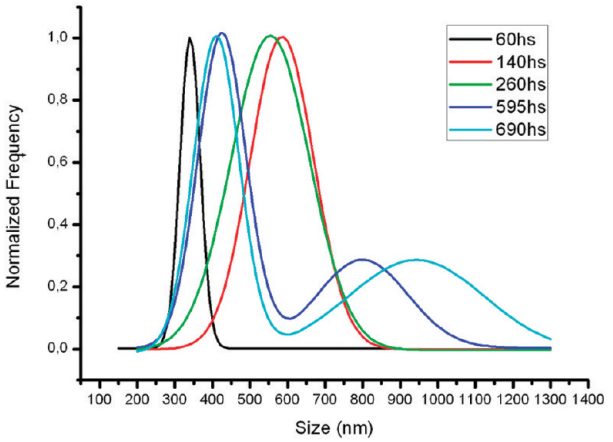

Figure 7. Size distribution of colloids shown in Figure 6A−E. Gaussian fits of the histograms are plotted to aid in visualization.

lowest-energy interaction between chains is produced when the total dipolar moment of one chain is oriented in the opposite direction to that of the total dipolar moment of their first neighbors.[25,29]

Secondary particles were studied by SEM to obtain the colloidal size distribution as a function of reaction time (see Figure 6A−E). SEM images were obtained from samples deposited on conductive tape. A mean number of 900 particles per sample were measured to acquire robust statistics for size distribution. The size dispersion showed changes from a sharp unique peak distribution at early stages to two broad peaks shifted to larger diameters taken after reaction for 595 and 690 h (Figure 7). Moreover, a decrease in the size of small particles and an increase in the diameter of large particles were observed; in other words, a classical ripening process takes place.

Since the monodispersion of colloid size is only found at initial stages of precipitation, colloidal crystals are feasible for appearing at these stages. Many routes were reported for the colloidal crystal assembly, sedimentation in a gravitational field,[30] self-assembly under physical confinement,[31] slow evaporation of colloid suspensions on vertical substrates,[32] etc. The simplest way is sedimentation, although it also involves several processes like settling, translational diffusion, nucleation, and growth. The number of layers is not controlled in this technique, but a variation introduced by Colvin et al.[32] contributed to the solution of this problem. However, it is still a slow process which has a duration from weeks to months. Physical confinement provides a faster method for controlling the number of layers, but it implies the use of continuous sonication to achieve thermodynamic equilibrium. Different methods with their own advantages and disadvantages have been reviewed.[33,34]

The chosen method for this work is sedimentation by gravity, in which there are two forces acting in the system: the gravity pushing the colloids to the bottom and the solvent viscosity stopping their sedimentation. A low solvent viscosity does not stop the sedimentation of the colloids, and it may cause a disordered phase. A large viscosity makes it difficult for the particles to reach the bottom and to form crystals. In the route

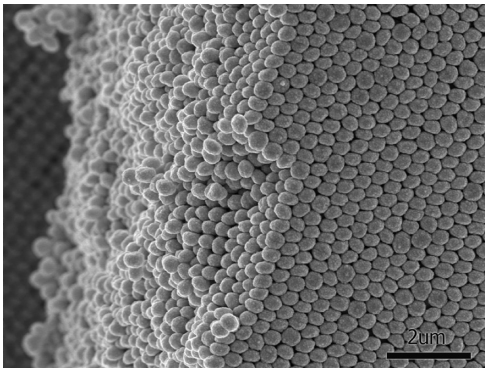

Figure 8. Top and lateral SEM views of colloid packing.

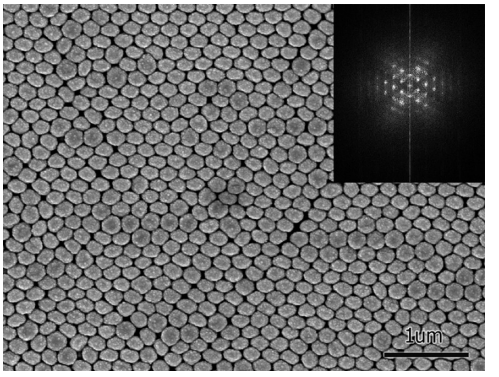

Figure 9. Top view of ordered colloids. The inset shows a fast Fourier transform of the image showing long-range order.

used in this work, the ethanol viscosity (1074 mPa at 25 °C)[35] is enough to decrease the sedimentation rate of small colloids and to obtain colloidal crystals. The obtained structures were observed by SEM; order is found on the surface and in depth (Figure 8), and a long-range order packing of spheres is observed by Fourier transform in Figure 9.

4. Conclusions

In this work, an alcoholic synthesis approach to obtaining hierarchical structures was used, taking advantage of the strong complexing action of DEA over Zn(II) ions, the low water content, and the strong dielectric moment of wurtzite nanocrystals. The first two facts control the hydrolysis and condensation processes, while the third one allows the formation of spherical colloids. The slow process of nano building block formation allows generation of spherical colloids with aggregation controlled by reaction. Colloids were deposited at a slow rate to form hierarchical colloidal crystals. The technique reported in this work exhibited some advantages in comparison with those of earlier works:[10] the monodisperse colloids were produced in a one-pot reaction, and the sedimentation and evaporation processes were conducted at room temperature. It is important to note that room temperature has preserved the nanocrystal dimension, and it has avoided thermal cracking of capping agents (acetates) protecting the surface of the crystals.

The influence of reaction time was studied by XRD and SEM. XRD showed an increase in crystal size with reaction time, and different growth rates on crystallographic direction were observed, according to previously reported theoretical and empirical

(29) Titov, A. V.; Král, P. *Nano Lett.* **2008**, 8, 3605.
(30) Mayoral, R.; Requena, J.; Moya, J. S.; López, C.; Cintas, A.; Miguez, H.; Meseguer, F.; Vázquez, L.; Holgado, M.; Blanco, A. *Adv. Mater.* **2004**, 9, 257.
(31) Park, S. H.; Qin, D.; Xia, Y. *Adv. Mater.* **1998**, 10, 1028.
(32) Jiang, P.; Bertone, J. F.; Hwang, K. S.; Colvin, V. L. *Chem. Mater.* **1999**, 11, 2132.
(33) Xia, Y.; Gates, B.; Yin, Y.; Lu, Y. *Adv. Mater.* **2000**, 12, 693.
(34) Zhang, J.; Sun, Z.; Yang, B. *Curr. Opin. Colloid Interface Sci.* **2009**, 14, 113.
(35) Lide, D. R., Ed. *CRC Handbook of Chemistry and Physics 2007*, 87th ed.; Taylor and Francis: Boca Raton, FL, 2007.

results. SEM showed the classical ripening process, starting with monodisperse colloids and reaching a broad size distribution. These hierarchical colloids exhibit promising applications for the development of new photonic devices because of the high dielectric constant of ZnO and the possibility of tuning the band gap of the nano building blocks.

Acknowledgment. We thank CONICET and the YPF Foundation for financial support, L. I. Pietrasanta and M. C. Marchi (CMA-UBA) for SEM assistance, R. Tarulla for FTIR measurements, Manuela Kim, Ismael Fábregas, and Myriam Aguirre for fruitful discussion, and C. Morales (OTMO) for assistance with the artwork.